applied sciences

MDPI

Article

The First Stages of Chemical and Electrochemical Aniline Oxidation—Spectroscopic Comparative Study

Zuzana Morávková *, Ivana Šeděnková and Patrycja Bober

Institute of Macromolecular Chemistry, Czech Academy of Sciences, Heyrovsky Sq. 2, 168 06 Prague, Czech Republic; sedenkova@imc.cas.cz (I.Š.); bober@imc.cas.cz (P.B.)

* Correspondence: moravkova@imc.cas.cz

Received: 20 February 2020; Accepted: 12 March 2020; Published: 19 March 2020

Abstract: There are several types of aniline oligomers that can be formed in the early stages of aniline oxidation: linear oligomers with repeating units joined in *para* positions, and various branched and polycyclic oligomers, being the two most important groups. The fraction of these different oligomeric groups depends upon the reaction conditions of aniline oxidation. The aim of this study was to analyze the first products of the chemical and electrochemical oxidation of aniline at the (starting) pH 1 and 7, in order to specify the conditions of the formation of phenazine-like oligomers, and to test the theory that they have an important role in polyaniline film formation. We have confirmed that phenazine-like oligomers do not form at pH 1, neither in the chemical nor the electrochemical oxidation of aniline; however, they form in both chemical and electrochemical oxidation of aniline at pH 7. Phenazine-like oligomers are thus definitely not necessary intermediates for PANI film formation, not even in the chemical polymerization of aniline. Finally, the redox behavior of phenazine-like oligomers was demonstrated in a medium at pH 1.

Keywords: polyaniline; aniline oligomer; electrochemistry; FTIR; SERS

1. Introduction

Polyaniline (PANI) is one of the most studied conducting polymers. It has a wide range of applications, including wastewater processing [1,2], catalysis [2], sensing [3–6], biomedical [5,7,8], optical [9] and electrochemical [9–13] applications. Many of these areas require PANI in the form of a thin film.

PANI and aniline oligomer (AO) thin films can be prepared by in-situ chemical [14–16] or electrochemical [15,16] polymerization. In both cases the type of formed product depends upon the initial pH [17,18]: In an acidic medium, the linear PANI chain is formed with aniline units coupled exclusively in the *para* positions [16,17,19–22]. On the other hand, in neutral or basic media, *ortho*-coupling becomes possible in addition to *para*-coupling, which leads to a formation of a mixture of various AO structures [19,20,22,23].

The first stages of aniline oxidation influence the morphology of the obtained PANI powders and films [24]. At low pH, the granular morphology of PANI is observed on PANI powder samples [17,20,24], while the films display the brush-like ordering of the PANI chains [15]. The chemical oxidation of PANI in a neutral medium or a medium of moderate acidity leads to the formation of nanotubes and nanorods. There are several theories explaining the mechanism of the linear structure formation [17,20,24,25]. In basic media, hollow microspheres of AOs are formed [24]. However, in this case, the morphology is caused more likely by the poor solubility of aniline in the basic medium than by the properties of AOs.

Specific AO species based on the *N*-phenylphenazinium cation were believed to be responsible for the tubular morphology formation and film adherence to the substrates [17,20,26–28]. However, aniline dimer was proven to be the adsorbing species in electrochemical aniline oxidation at any

pH [18]. The PANI film obtained by the in-situ chemical oxidation of aniline at very low pH also seems to contain no *N*-phenylphenazinium cation structures. However, as only finished film was studied in this case, Raman spectra without surface-enhanced Raman scattering (SERS) enhancement brings restricted information about the first products [29]. These findings lead to the question whether the *N*-phenylphenazinium cation-based AOs play any role in film formation within in-situ chemical aniline oxidation.

If the absence of the *N*-phenylphenazinium cation in the PANI films prepared by in-situ chemical polymerization is proven, the in-situ chemical PANI film preparation must then be equal to the electrochemical method from the PANI-chain linearity point of view. Beside this, there are other relevant factors in the chemical and electrochemical preparation of PANI films that influence the applicability of these methods: (1) Electrochemical PANI film preparation requires a conducting substrate that serves as a working electrode in the polymerization cell. The in-situ chemical polymerization of aniline operates at any surface, including e.g., glass, textiles, the solution–air interface, etc. [14,16]. (2) In the case of the electrochemical method, PANI is only formed at the electrode, while during the chemical method, PANI also forms as a precipitate in the bulk solution, increasing reactant consumption for a unit of surface area of formed PANI film [14].

Although chemically prepared AOs have already been studied by various methods [27,28,30], a SERS study of the reaction kinetics has not been performed yet. The presence of *N*-phenylphenazinium cation-based AOs during chemical oxidation has been proven only by its detection in fully formed film [28]. In the case of the electrochemical oxidation of aniline, only studies in low pH and dimerization are available [15,22,31–33]. Studies of electrochemical aniline oxidation at neutral pH are also limited simply to the detection of *N*-phenylphenazinium cation [18,34].

In this work, we thoroughly study and compare the first products of both the chemical and electrochemical oxidation of aniline at pH 1 and 7 with the methods of in-situ and ex-situ FTIR and Raman spectroscopies. The role of phenazine-like oligomers in the process of aniline oxidation is better specified.

2. Materials and Methods

2.1. Chemicals

Aniline (≥99.5%) and sulfuric acid (≥97.5%) were purchased from Sigma-Aldrich. Sodium sulfate and ammonium persulfate (APS) were obtained from Lach-Ner. All chemicals were used as received, without any further purification. Ultrapure Q-water ultra-filtered in a Mili-Q Gradient A10 system (Millipore, Molsheim, France) was used for the preparation of solutions.

2.2. Chemical Preparation

The chemical oxidation of 0.05 M aniline with 0.0625 M APS was performed in an aqueous solution of 0.1 M sulfuric acid (pH 1) or 0.1 M sodium sulfate (pH 7) at room temperature. Both monomer and oxidant were separately dissolved in the required solution to 50 mL, then these solutions were mixed to start the oxidation of aniline. The reaction mixture was left at rest to polymerize. During the polymerization the pH and temperature of the reaction mixture were recorded using the HI-4221 Research Grade Bench pH and ORP Meter (Hanna Instruments) to assess the progress of reaction. The open circuit potential (OCP) measurements were conducted in a two-electrode setting with a platinum working electrode and Ag/AgCl counter electrode.

Suitable glass windows for UV—vis and the modified electrode (see below) for SERS measurement were placed in the reaction mixture. The supports were removed from the reaction mixture at given times, rinsed with water or 0.1 M sulfuric acid for the pH 7 and pH 1 experiments, respectively, and the film of AOs or PANI was characterized by UV—vis and SERS spectroscopy.

2.3. Electrochemical Preparation

Electrochemical oxidation of aniline was carried out in a Raman spectroelectrochemical cell in an aqueous solution of 0.05 M aniline and 0.1 M sulfuric acid (pH 1) or 0.1 M sodium sulfate (pH 7). The cell consisted of the SERS golden working sheet-electrode, platinum wire counter electrode and Ag/AgCl pseudo-reference electrode. All potentials are given versus the Ag/AgCl pseudo-reference electrode. A 1 mm thin glass optical cuvette was used as a vessel. The usage of this optical cuvette enables us to focus the Raman laser on the surface of the electrode, and to study the electrochemically-formed films of AOs and polyaniline in situ. The potentiodynamic method of PANI deposition was applied. For further Raman spectroelectrochemical (SEC) study, 0.1 M sulfuric acid solution was used as an electrolyte.

2.4. Electrochemistry

The electrochemical measurements were controlled by a Bio-logic potentiostat/galvanostat VSP300. During the in-situ Raman spectroelectrochemistry (SEC), the potential was changed at the rate of 10 mV/s for the measurements with 785 nm excitation, and 0.7 mV/s for the measurements with 633 nm excitation; leading in both cases to the data density of 1 spectrum per 0.04 V range.

2.5. FTIR Kinetics

The chemical polymerization of aniline was studied in the aqueous solutions of 0.1 M sodium sulfate and 0.1 M sulfuric acid. The oxidation of the aniline monomer was followed in situ by attenuated total reflection (ATR) infrared spectroscopy, using a Thermo Nicolet NEXUS 870 spectrometer with an MCT nitrogen-cooled detector. The droplet (0.75 µL) of 0.05 M aniline solution was placed on the surface of the ZnSe crystal, and the same amount of 0.0625 M APS solution was added [35]. The spectra were recorded at the resolution of 4 cm^{-1}, and 32 scans were accumulated for each spectrum. The spectra were measured continuously, where each spectrum took 12.75 s. The spectrometer was purged with dry air.

2.6. Raman Spectroscopy

Raman spectra were collected on a Renishaw inVia Reflex Raman spectrometer (Leica DM LM microscope; objective magnification ×50) with a HeNe 633 nm laser (holographic grating 1800 lines mm^{-1}) and diode 785 nm laser (holographic grating 1200 lines mm^{-1}).

Where relevant, a selected spectral region was deconvoluted with gaussian peaks on a linear baseline using an octave script.

2.7. SERS Substrate Preparation

The SERS substrates were prepared by the following procedure, based mainly on the work of Liu et al. [36]: The gold sheet electrodes were flame cleaned at the point of melting, and then by potential cycling in 1 M sulfuric acid. Then it was cycled in 1 M potassium chloride in hydrochloric acid tuned to pH 1 (0.1 M hydrochloric acid). The cycle consists of 2 V/s ramp form −0.6 V to 1 V, 1 s hold at 1 V, 2 V/s ramp from 1 V to −0.6 V and 2 s hold at −0.6 V; it is repeated ca 200 times depending on the size of the electrode. The counter electrode is platinum sheet, and Ag/AgCl is used as pseudo-reference.

3. Results

In order to compare the chemical and electrochemical oxidation of aniline as reliably as possible, we have brought some typical conditions of chemical oxidation to our electrochemical experiment, and vice versa. The electrochemical oxidation of aniline is typically conducted in a strongly acidic medium (0.1 M sulfuric acid—pH 1, in our case) and the pH is maintained throughout the reaction [15]. The chemical oxidation of aniline, on the other hand, is initiated in media with acidity varying from ca pH 2 to 8 [17,24]. The pH also changes during the chemical oxidation of aniline with APS as sulfuric acid is a byproduct.

In our experiment, we start both electrochemical and chemical aniline oxidations in 0.1 M sulfuric acid (pH 1) and 0.1 M sodium sulfate (pH 7). The sodium sulfate was chosen as an electrolyte for the electrochemical experiment to keep the condition of electrochemical polymerization close to the conditions of chemical polymerization.

3.1. Kinetics of Chemical Aniline Oxidation at pH 1 and 7

The course of chemical oxidation of aniline can be followed by temperature [37], OCP [21] and pH [37], providing information on the reaction rate and distinguishing its phases (Figure 1).

The oxidation of aniline started at pH 1 has an induction period of ca 3 min. Then, the temperature and pH change dramatically (Figure 1b,c). This is connected with the formation of growing chains in the pernigraniline form. After another ca 10 min, potential drops and the decrease of pH slows down (Figure 1a,b) as the transformation of pernigraniline to emeraldine becomes the prevailing reaction. Temperature, reflecting changes in the bulk rather than on interfaces in contrast to pH and OCP, starts dropping almost an hour after the beginning of the experiment (not shown). This demonstrates the fact that oxidation of aniline in acidic medium is faster at interfaces than in solution.

When starting at pH 7, the progress of the reaction seems to be much faster (Figure 1). The potential drops to zero within the first minute, and then increases gradually during the next ca 15 min. Then the electrodes are probably passivated, as only artifacts are observed in the OCP measurement. The pH drops during the first 15 min, and then the rate of decrease slows down. As the temperature follows the same trend as pH and potential, we can assume that for this pH range the rate of aniline oxidation is similar on interfaces and in solution.

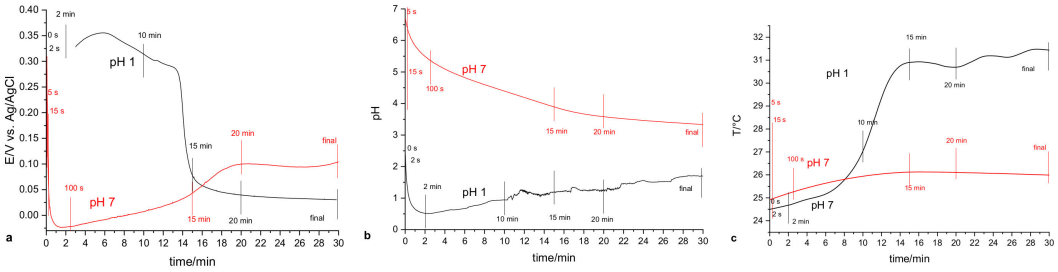

Figure 1. Open circuit potential (OCP) (**a**), pH (**b**) and temperature (**c**) profile of the chemical oxidations of aniline at starting pH 1 and 7.

3.2. FTIR Kinetic Study of the Chemical Oxidation of Aniline

To study the chemical oxidation of aniline in detail, the molecular structure of the products was followed in situ by ATR-FTIR spectroscopy. The spectrum of the reaction mixture, measured before any changes could be observed (i.e., the spectrum of reactants), was subtracted from all spectra. The differential spectra are presented in the Figures 2 and 3; complete band assignment is summarized in Table 1.

In the neutral medium (pH 7), the oxidation of aniline starts immediately after the addition of the APS solution to the aniline solution. The main bands observed at 1509 cm^{-1} and 1586 cm^{-1} are assigned to the stretching vibration of the –C=C– bond of quinonoid and benzenoid rings, respectively. The intensity of the band connected with the quinonoid ring is significantly lower than the intensity of the benzenoid band. Two bands typical for nanostructured PANI material are observed at 1445 cm^{-1} (skeletal vibration of the substituted aromatic ring) and 1415 cm^{-1} (phenazine-like ring stretching vibrations).

The band at 1707 cm^{-1} observed in several of the first spectra corresponds to the stretching vibration of the carbonyl group on the quinone ring. The intensity of the band decreases during the proceeding reaction. The band assigned to the C–N bond stretching next to the aromatic ring at 1365 cm^{-1} is shifted from the typical position at 1374 cm^{-1} expected in PANI. This can be attributed to the 1,2,4-substituted ring formation instead of the typical 1,4-substituted ring. The higher intensity of the

band at 861 cm^{-1} (out-of-plane C—H bending vibration on the aromatic ring), together with the band at 846 cm^{-1}, signifies the higher fraction of the tri-substituted aromatic rings in the molecular structure.

As the oxidation of aniline proceeds, the position of the bands remains practically unchanged, and the only difference between bands in the first spectrum and the spectrum measured after 15 min of the reaction is their intensity.

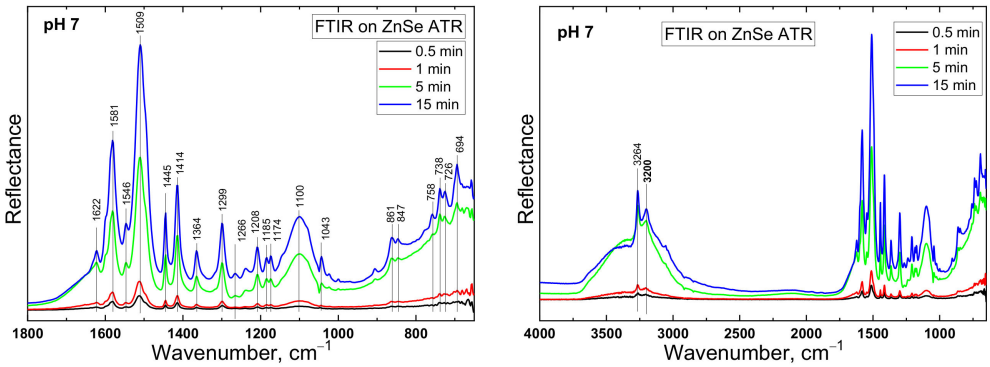

Figure 2. Selected spectra representing the evolution of attenuated total reflection (ATR) Fourier transform infrared (FTIR) spectra of aniline oxidation at pH 7 on ZnSe crystal. The spectrum of the reaction mixture was subtracted from each spectrum.

Table 1. Assignment of the FTIR bands in the in-situ FTIR experiment at pH 7.

Acid	Assignment	Product	References
3264	ν(N–H)	Hydrogen bond to C=O of *p*-benzoquinone	[35]
3200	ν(N–H)	Hydrogen bonded to sulfonic group	[35]
1622	δ(NH) of primary aromatic amines; ν(C=O) quinonoid	AO, monomer	[38]
1581	ν(–C=C–) of the Q ring	linear chain	[39,40]
1546	ν(C–C) of the B ring or phenazine-like unit	AO	[39]
1509	ν(–C=C–) of the B ring	linear chain	[39]
1445	ν(ring) of the substituted aromatic ring	Phenazine-like structures	[39,41,42]
1414	ν(phenazine ring), ν(C–C) next to the imine group	Phenazine-like structures	[39,41,42]
1365	ν(C=N) next to the aromatic ring	1,2,4-substituted ring	[38]
1299	ν(arom. amines)	*p*-benzoquinone, phenazine-like structures	[38]
1266	ν(C–N), δ(C–H) in the Q ring, ν(C–O)	primary amines, *p*-benzoquinone, phenol	[17,38,39]
1208	ν(C–N)	primary amines	[17]
1185/1174	δ(C–H) in plane	quinone diimine structures	[39]
1100	ν(SO_4^{2-})	ammonium sulfate	[43,44]
1043	ν(SO_4^{2-})	sulfated aromatic rings	[43,44]
861	γ(C–H) out of plane	tri-substituted aromatic ring	[45]
847	γ(C–H) out of plane	di-substituted aromatic ring	[45]
758	γ(C–H)	linear chain	[46]

The evolution of spectra measured during aniline oxidation in sulfuric acid (pH 1) is significantly different (Figure 3, Table 2). The intensive bands appearing earliest in the differential spectrum

are connected with water (1630 cm^{-1}), aniline (1499 cm^{-1}) and APS (1048 cm^{-1}). The fact that the bands of reactants and water are present, even in the differential spectra, can be assigned to two factors: (1) The droplet of the reaction mixture spreads wider on the ATR crystal during first minute of the oxidation reaction, which influences the subtraction, and (2) the reactants are adsorbed on the crystal surface. Both factors play their role. The presence of water bands is exclusively caused by the higher area of the droplet–crystal interface. On the other hand, due to the adsorption of the reactants, the intensities of the bands from aniline and APS are considerably higher than expected based on the reactant spectra. We do not observe this behavior in the evolution of spectra measured in the salt solution (pH 7), as the first products are formed fast enough to cover the crystal–solution and solution–air interfaces, and stabilize the shape of the droplet.

The first distinguishable bands which are not connected with the reactants are observed after 2 min of oxidation. The band at about 1110 cm^{-1} is assigned to the vibration modes of ammonium sulfate, the product of the APS decomposition. The broad, weak band found at about 1250 cm^{-1} is most probably connected with the vibration of amine groups in the aromatic amines.

After 2 min, the band at 1571 cm^{-1} (stretching vibration of quinonoid rings), the weak, broad band at about 1500 cm^{-1} (vibration of benzenoid ring in the PANI structure), and bands at 1376 cm^{-1} (imine structure in pernigraniline), 1285 cm^{-1} and 1260 cm^{-1}, appear. The broad band at about 1100 cm^{-1} and a sharp band at 1047 cm^{-1} are connected with formation of ammonium sulfate. The intensity ratio of the quinonoid and benzenoid ring stretching bands corresponds to the higher content of the quinonoid rings observed in the first stages of chemical aniline oxidations [17]. A shoulder on the broad band at 1490 cm^{-1}, at about 1460 cm^{-1} corresponding to pernigraniline [46,47], is also observed.

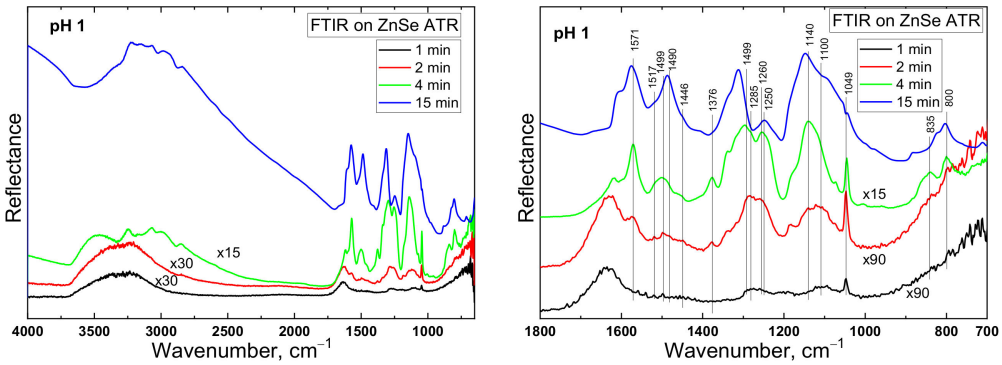

Figure 3. Selected spectra representing the evolution of ATR FTIR spectra of aniline oxidation at pH 1 on ZnSe crystal. The spectrum of the reaction mixture was subtracted from each spectrum.

The main bands described above remain present also after 4 min of polymerization, with their positions slightly shifted. The band of quinonoid ring stretching at 1571 cm^{-1} is sharp, and one of the most intensive in the spectrum. The band linked to the benzenoid ring is broad, with its shoulder at about 1460 cm^{-1}. The band at 1376 cm^{-1} of the imine structure (pernigraniline) [47,48] is well pronounced. The maxima of the broad band between 1200 and 1300 cm^{-1} are shifted to 1296 and 1254 cm^{-1}. The maximum of the ammonium sulfate band is at 1140 cm^{-1}. The sharp band linked to the sulfate ions is at 1050 cm^{-1}. The bands of out of plane vibration are shifted to 840 and 800 cm^{-1}. In this spectrum, the structure of the C–H and N–H stretching bands in the region 3400–2800 cm^{-1} is developed. The bands have maxima at 3245, 3071, 3003 and 2849 cm^{-1}. The maximum at 3465 cm^{-1} is connected with the OH vibration of water.

Table 2. Assignment of the FTIR bands in the in-situ FTIR experiment at pH 1.

Acid	Assignment	Product	References
1571	ν(−C=C−) of the Q rings	neutral AO	[39,40]
1517	ν(C−C) + δ(C−H)	doped dimer	[39]
1499	ν(−C=C−) of the B rings	neutral AO	[40]
1490	ν(−C=C−) of the B rings	protonated PANI chain	[40]
1460 sh	ν(ring) substituted aromatic ring	pernigraniline	[47,48]
1376	ν(C=N) next to the aromatic ring	pernigraniline	[47,48]
1312/1338	ν(C≈N)	PANI chain/AO (delocalization length)	[39]
1302	ν(C−N)	secondary aromatic amines	[45]
1285	δ(N−H) + ν(C−N)	Primary amino group	[38]
1260	δ(C−H) in the Q ring, ν(C−N), ν(C−O)	Primary amino group in AO, *p*-benzoquinone	[17,38,39]
1245	ν(C−N^+)	PANI salt	[49]
1148	ν(=NH^+−)	protonate PANI chain	[38,39]
1100	ν(SO_4^{2-})	ammonium sulfate	[43,44]
1049	ν(SO_4^{2-})	sulfated aromatic rings	[43,44]
835	γ(C−H)	1,2-disubstituted ring	[45]
800	γ(C−H)	1,2-disubstituted ring	[39]

The spectra evolve rather evenly afterwards, until ca 15 min reaction time. The overall intensity increases significantly, and the absorption above 2000 cm^{-1} is observed, typical of the conducting form of PANI. The intensity of the benzenoid band increases faster than the intensity of the quinonoid band, corresponding to the transformation to the emeraldine form of PANI. The position of the benzenoid bands is then shifted to 1488 cm^{-1}, while the position of the quinonoid bands remains at 1572 cm^{-1}. The band at 1376 cm^{-1} is suppressed, and only a shoulder remains. The intensive bands at 1312 cm^{-1} and the band at 1241 cm^{-1} are connected with delocalization of π-electrons, and are linked to the protonation of the PANI chain. The most intensive band at 1141 cm^{-1} is assigned to the vibration of the =NH^+− group. The band at 801 cm^{-1} in the region of the out-of-plane vibrations remains in the spectrum. In general, the differential spectrum obtained after about 15 min of the oxidation reaction is in accordance with the spectrum of emeraldine PANI film prepared in the oxidation reaction in sulfuric acid.

3.3. UV—Visible Absorption Spectroscopy of Chemically Oxidated Aniline

In contrast to FTIR, UV—visible absorption and SERS kinetics of the chemical oxidation of aniline could not be conducted in situ, as the solution becomes opaque during the reaction, and the bulk material rather than the film is analyzed. The chemical oxidation of aniline was conducted in a wide beaker. Glass slides and SERS substrates were introduced in the medium at the very beginning. Based on the kinetics, certain times were selected for removal of the substrates from the reaction medium.

The spectra were normalized, and in the case of pH 7 also shifted for clarity, the total absorbance of the sample was strongly dependent on the film thickness.

Significant differences are observed between UV—Vis absorption spectra obtained on glass substrates removed from the reaction mixtures at pH 1 and 7 at various times (Figure 4). Whereas in the strongly acidic medium, PANI in the emeraldine (15 min, final) [41,50–53] and pernigraniline (2 min, 10 min) [48,52] salt form is observed. The evolution of the UV—Visible absorption spectra of the product formed at pH 7 are more complex. After 15 s of reaction, a spectral shape corresponding to emeraldine salt is observed. After 100 s, a relatively narrow band at 425 nm appears, which corresponds to the charged phenazine-like AOs [54,55].

This band is then present till the end of the reaction, with only minor shifts in position. The shoulder at 480 nm observed in the spectra obtained after 15 and 20 min of reaction is attributed to radical cations of aniline-type dimer [54]. The soluble dimer intermediates were clearly not washed off properly after the substrate removal from the reaction mixture.

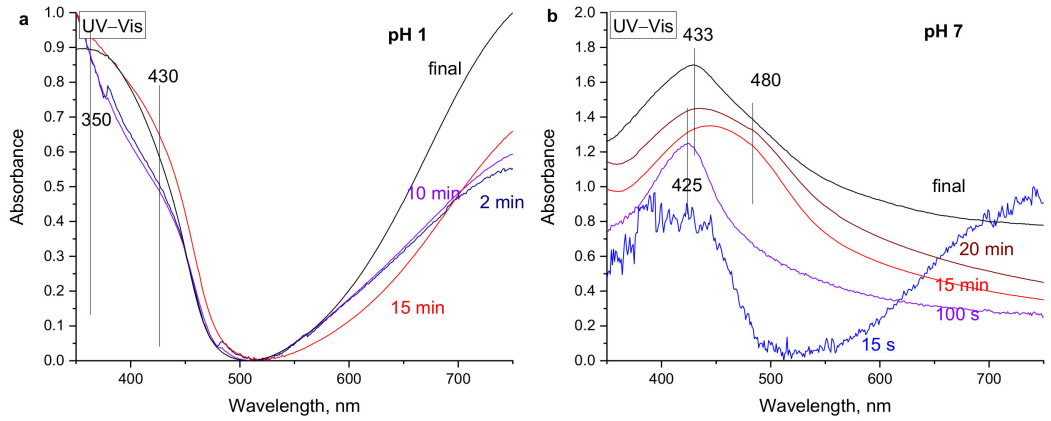

Figure 4. UV-Visible absorption spectra of chemically oxidized aniline films on glass removed from the reaction mixture of starting pH 1 (**a**) and 7 (**b**) at various times after mixing. The spectra are normalized for clarity.

3.4. Raman Spectra Obtained on SERS Electrodes Removed from the Media at Different Times of Chemical Aniline Oxidation

Raman spectra of the products of aniline oxidation on SERS electrodes at our starting pH 7 excited with the 785 nm laser line (Figure 5a, Table 3), vaguely resemble those of emeraldine salt. The 785 nm excitation line is in resonance with charged emeraldine and pernigraniline-like structures, making the semiquinonoid (1600 cm^{-1}) and quinonoid rings (1625 cm^{-1}) with charged nitrogen structure (~1370 cm^{-1}) dominant in the spectrum.

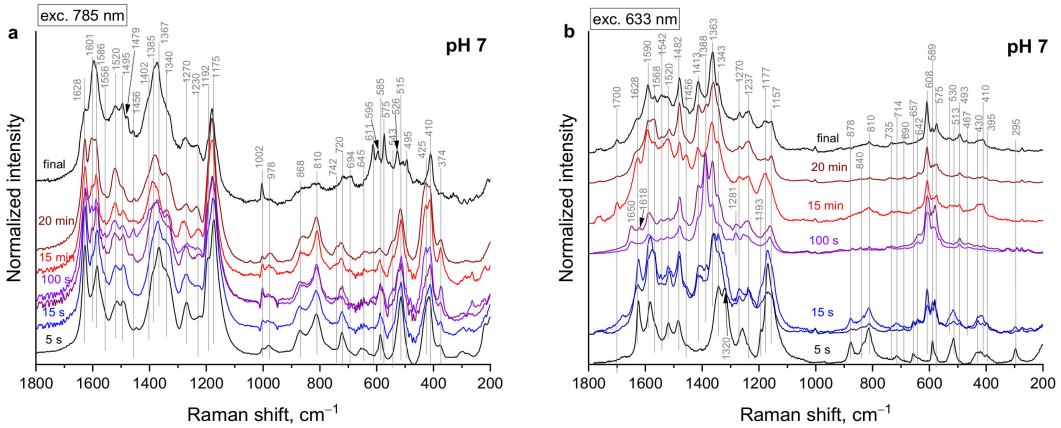

Figure 5. Raman spectra of gold, surface-enhanced Raman scattering (SERS) electrodes removed from the reaction mixture of starting pH 7 at various times. Excitation 785 nm (**a**) and 633 nm (**b**).

The phenazinium cation-based AOs are resonantly enhanced by the laser line at 633 nm [28]. Their typical spectral profile strongly dominated by the bands at 1388/1363 and 608/575 cm^{-1} is clearly observed (Figure 5b, Table 3) [28,34]. However, they appear after ca 100 s of reaction, not immediately (Figure 5). A C=O stretching band of benzoquinone-based AOs is observed at 1650 cm^{-1}. The spectra obtained after 5 and 15 s of reaction reflect the formation of mainly linear AOs (typical bands at 1628, 1590, 1343 and 1177 cm^{-1}). This might mean that phenazinium cations are formed later on, or that the phenazine-like AOs is protonated at later phases of the reaction after the pH drops (Figure 1b). As the

resonant enhancement is operative only for the protonated species, the neutral *N*-phenylphenazine structure may not be detected. At later stages of the reaction, a complex spectrum of the AO mixture is observed: typical bands of *N*-phenylphenazinium cation (1388/1363, 608, 575 cm^{-1}) and linear emeraldine (1628, 1590, 1343 and 1177 cm^{-1}) are observed.

Table 3. Summary of observed Raman peaks—peak positions are rounded to 5 cm^{-1}.

633 nm	785 nm	Assignment	Typical Product	Reference
1700		C=O stretching (overoxidation)		[43]
1650		n(C=O) BQ	degradation products	[43,56]
1625	1625	n(ring) of the B ring next to the Q ring in a Q structure	linear chain, monomer	[39,49,57–59]
1620		n(C-N)	monomer	[60]
1605	1600	n(ring) of B ring in the SQ structure	linear chain	[46,57,58,61]
1595		SQ n(ring)	linear chain	[39,57]
1585	1585	n(ring) of the B ring in the B structure	linear chain, aniline cation radical, phenazine-like structure	[28,46,49,57,60,61]
1565	1555	n(ring) B	linear chain bases	[46,57,62]
1540	1535	n(ring) B	end-chain B	[63,64]
1520	1520	d(*N*-H)	linear chain	[49,57,58,61]
1505		d(*N*-H)	Charged phenazine-like structures	[65]
1490	1495	n(C=N)	emeraldine base	[46,57,66]
1480	1480	n(C=N)/d(C-H) + n(C-C)	emeraldine or pernigraniline base, aniline cation radical	[46,57,60,66]
1475/1485		n(C~N)	Charged phenazine	[28]
1470		n(C=N)	linear chain bases	[28,46,66]
1460	1455	n(C=N)	linear chain bases, phenazine-like structure	[46,63,66]
1450	1450	d(C-H) + n(ring)	linear chain	[46,59]
1410/1425	1400/1415	n(C~N)/n(ring) Q/neutral phenazine	linear chain bases	[46,57,65]
1390	1385/1390	n(C~N), polaron pair	highly doped linear chain, phenazine-like structure	[59,66]
1380	1380	n(C~N), localized polaron	linear chain, aniline cation radical	[59,60]
1365	1370	n(C~N), localized polaron	phenazine-like structure	[28]
1335/1355	1335/1340	n(C~N), delocalized polaron; d(C-H) B	linear chain/base	[46,49,57,58,61]
1320		n(C~N), delocalized polaron	linear chain	[49,57,58,61]
1280		d(C-H) B	linear chain, aniline	[46,60]
1260/1270	1270	d(C-H) Q + P	linear chain bases, phenazine-like structure	[46]
1230/1235	1230/1235	n(C-N), B or polaron	linear chain	[46]
	1225	n(C-N), B or polaron	linear chain	[46,57,59,67]
1185	1190	d(C-H), Q or polaron pair	linear chain, aniline cation radical	[49,57,58,60,61]
1175/1160	1175	d(C-H), B and SQ	linear chain	[46,57]

Table 3. *Cont.*

633 nm	785 nm	Assignment	Typical Product	Reference
1150/1155		d(C-H), Phz	benzenoid ring, phenazine-like structure	[18,28,46,57]
1055		H2SO4	H2SO4	[68]
1045	1035	H2SO4, aniline	H2SO4	[60,68]
	1010	H2SO4	H2SO4	[68]
1010	1010	H2SO4	H2SO4	[68]
1000	1000	H2SO4, aniline	H2SO4, aniline + +*	[60]
960	970/980	d(ring), B or polaron	linear chain	[46]
880	880	d(ring), Q or polaron pair	linear chain	[46]
	868	d(ring), Q or polaron pair	linear chain	[46]
840	850	d(ring), Q or polaron pair	linear chain	[58,61]
	830	d(ring)	linear chain	[46]
810	810	d(ring)	linear chain, aniline	[57,60–62,69]
	805	d(ring)	linear chain	[57,61,62,69]
735	740	d(C=*N*-C)	linear chain bases	[46,57]
715	720	d(C=*N*-C)	linear chain bases	[46,57]
690	695		phenazine-like structure	[65,70]
655	660	g(ring) SQ	linear chain	[39]
640	645	g(ring), localized polaron	linear chain	[49,58]
610	610	g(ring), Phz	phenazine-like structure	[28,58,61]
590	595		phenazine-like structure	[65,70]
590	585	g(ring), Q	linear chain	[46]
575	575	g(ring), polaron pair	linear chain bases, phenazine-like structure	[71]
550	545	g(ring)	linear chain, aniline	[60]
530	525	g(ring), Q or polaron pair	linear chain	[65,69,72]
515	515	g(*N*-H), Q or polaron pair	linear chain	[58,61]
495/505	495	g(ring)	linear chain bases, phenazine-like structure	[63,65,69]
465		g(ring)		
430	425	g(C-H), Q, t(C-*N*-C)	linear chain	[58,61]
410	410	g(C-H)	linear chain bases, phenazine-like structure	[58,61,63,69,73]
395	375	g(ring), Q	linear chain	[58,61]
295		g(C-*N*-C)	linear chain bases, phenazine-like structure	[69]

Raman spectra obtained on SERS electrodes removed at various times from the reaction mixture of aniline oxidation starting at pH 1 (Figure 6a, Table 3) are in line with the known pernigraniline route of aniline oxidation. At the beginning (electrode just dipped into the reaction mixture and rinsed with water right away) and after 2 s, the spectra corresponding to linear AOs (1627, 1584, 1390/1370, 1175 cm^{-1}) are observed [39,46,61] (Figure 7). Samples removed in the 2–20 min time window reflect the pernigraniline salt intermediate (1627, 1584, 1495, 1415, 1382, 1333, 1225, 1175 cm^{-1}) [63,67]. The final spectrum represents the emeraldine salt (1627, 1603, 1516, 1382/1333, 1175 cm^{-1}) [39,61]. In the spectra obtained with the 633 nm excitation line (Figure 6b, Table 3), the spectral features of the quinonoid pernigraniline structure (mainly 1582 and 1491/1482 cm^{-1}) are resonantly enhanced, thus, the spectrum

of the final film is not dramatically different from the spectrum obtained after 20 minutes – residual overoxidated units are still detected.

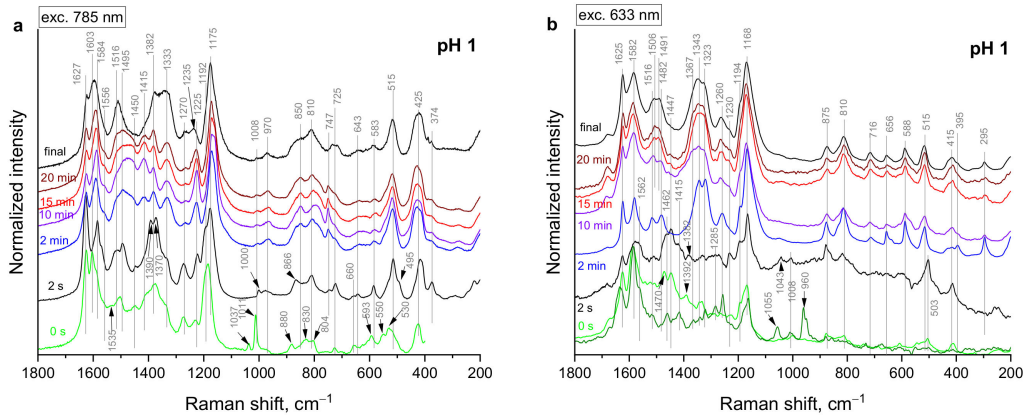

Figure 6. Raman spectra of gold SERS electrodes removed from the reaction mixture of starting pH 1 at various times. Excitation 785 nm (**a**) and 633 nm (**b**).

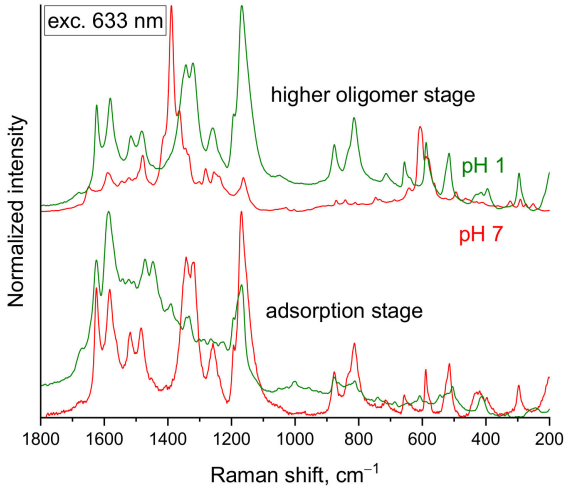

Figure 7. Raman spectra of gold SERS electrodes removed from the reaction mixture of starting pH 1 and 7 at adsorption stage (2 resp. 5 s after mixing) and at higher oligomer stage (1.5 resp. 2 min after mixing). Excitation 633 nm.

3.5. Raman SEC of the Aniline Oxidation at pH 7

Electrochemical oxidation of aniline was followed in situ by SERS SEC. The voltamperogram of the aniline oxidation at pH 7 (Figure 8a) shows only one oxidation peak at ca 0.4 V, and an oxidation ramp of aniline to cation radical, while the electrochemical oxidation of aniline at pH 1 shows only the aniline oxidation ramp (Figure 8b).

In the reduction phase, the pH 1 sample displays the weak reduction peaks of PANI at ca 0.45, 0.25 and −0.15 V, while the pH 7 reduction is flat, probably as the electrode is passivated by the AO layer.

The in-situ SERS SEC of aniline oxidation at pH 1 (Figure 9) was thoroughly described elsewhere [18]. For the purpose of this paper, this experiment is used as a reference of linear AO redox behavior.

The Raman spectra of the products of the electrochemical aniline oxidation at pH 7 (Figure 10) do not change much with potential; they mainly flatten due to increasing fluorescence typical for the non-protonated AO [17]. We will focus on the spectra excited with the 633 nm line, as it should lead to surface enhanced resonance Raman scattering (SERRS) enhancement of the charged phenazine-like

oligomers [28], while the 785 nm excitation line resonantly enhances the spectral features of the linear oligomer fraction. The small changes are visualized with potential dependency plots (Figure 11).

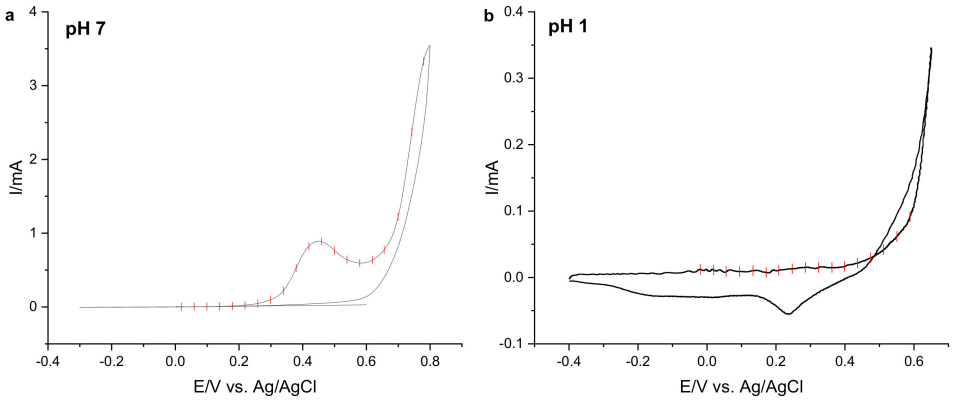

Figure 8. Electrochemical oxidation of aniline in aqueous medium of pH (**a**) 7 and (**b**) 1. Red marks separate potential ranges connected with one Raman spectrum.

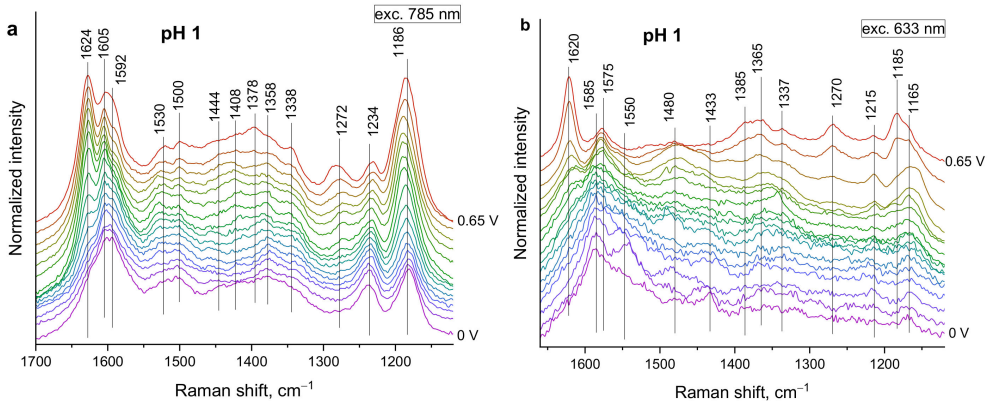

Figure 9. Raman spectra of gold SERS electrodes during the electrochemical oxidation of aniline in aqueous medium of pH 1 (excitation 785 nm (**a**) and 633 nm (**b**)).

The ring stretching mode shifts gradually from 1592 cm^{-1} (benzenoid ring (Table 3)) to 1598 cm^{-1} (charged semiquinonoid ring) (Figure 11a), implying gradual oxidation of the material deposited onto the electrode. The bands around 1170 cm^{-1} (C–H deformation on a benzenoid or semiquinonoid ring in a linear structure), 1592–1598 cm^{-1} (ring stretching of a semiquinonoid ring in a linear structure) and 1626 cm^{-1} (ring stretching of a benzenoid ring located next to a quinonoid ring in a linear structure) reach maximum intensity around 0.4 V—the maximum of the oxidation peak (Figure 11b). These bands correspond to the emeraldine form of protonated PANI.

The intensity of the bands at 1348 cm^{-1} (C–H bending on a benzenoid ring in a PANI base) and 1565 cm^{-1} (ring stretching of a benzenoid ring in a PANI base) increase at potentials above 0.4 V (Figure 11c), implying the formation of the oxidized but neutral PANI base.

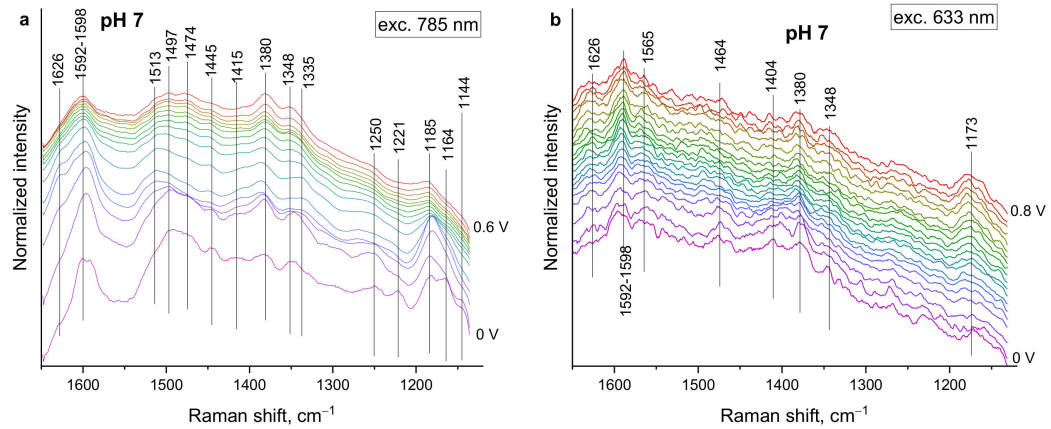

Figure 10. Raman spectra of gold SERS electrodes during the electrochemical oxidation of aniline in aqueous medium of pH 7 (excitation 785 nm (**a**) and 633 nm (**b**)).

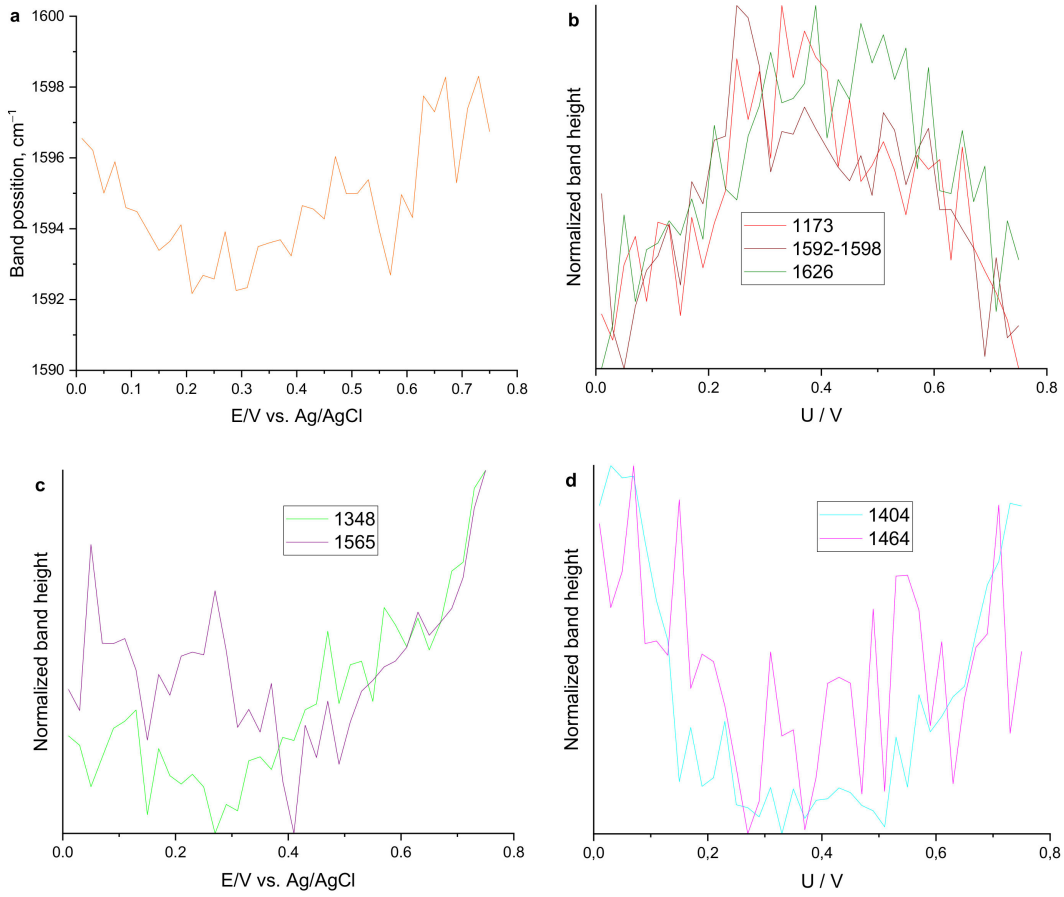

Figure 11. Potential dependencies of the position of the ring-stretching mode around 1600 cm^{-1} (**a**) and normalized band intensities of several changing bands during the electrochemical oxidation of aniline in aqueous medium of pH 7 (**b**–**d**). Excitation 633 nm.

The bands at 1404 cm^{-1} (quinonoid ring stretching of PANI base) and 1464 cm^{-1} (C=N stretching) have minimum intensity around 0.4 V (Figure 11d). This is probably the result of the higher intensity of other bands around 0.4 V.

From the in-situ aniline oxidation at pH 7 we can conclude that a layer of a mixture of AO structures is formed on the electrode. The linear fraction, that is electroactive, is responsible for the changes observed in the Raman spectra. The high background is probably due to the *ortho*-linked AOs that tend to display fluorescence if not protonated [17].

3.6. Raman SEC of the Film Prepared Electrochemically in Salt Solution, Conducted in 0.1 M H_2SO_4

Even if the AOs formed in pH 7 seem not to be very electroactive, this is not the case, as we illustrate by spectroelectrochemical study at pH 1. As the AOs become protonated, changes of the Raman spectra with potential as well as oxidation and reduction peaks in CV appear. At potentials below 0.3 V, we obtain a spectrum known for protonated phenazine-like AOs (*N*-phenylphenazinium cation) prepared chemically (Figure 9a). As the chemical oxidation of aniline is connected with a decrease of pH, the AOs must at some point become protonated. This is not the case for electrochemical oxidation – the *N*-phenylphenazinium cation features thus became visible after the electrolyte change. At higher potentials, the observed spectrum is identical to the spectra obtained during the electrochemical oxidation at pH 7. This process is probably connected with the oxidation peak around 0.3 resp. 0.2 V in the first resp. second oxidation run (Figure 12b). This peak has been previously connected with carbonyl defects [23,32], therefore, the AO probably contains both *N*-phenylphenazinium and benzoquinone unit in their structure (Figure 5b).

In a second oxidation run, the original Raman spectrum is not obtained. The main difference is the appearance of a band at 1394 cm^{-1} corresponding to C~N^+ stretching vibration, with a little more localized charge than in the case of the vibration peaking at 1371 cm^{-1}.

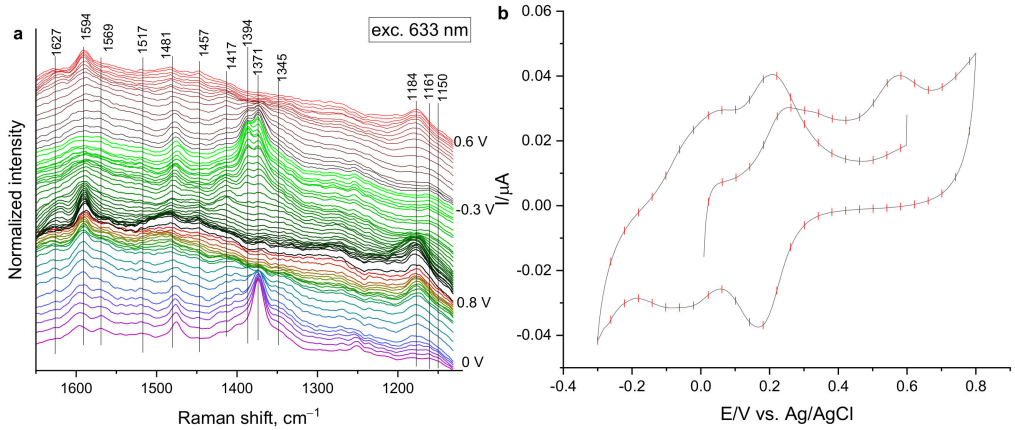

Figure 12. Raman spectra of gold SERS electrodes during the spectroelectrochemical study at pH 1 of the AO formed electrochemically in an aqueous medium of pH 7. Excitation 633 nm (**a**) and the corresponding CV (**b**). Red marks separate potential ranges connected with one Raman spectrum.

The less obvious changes are visualized by the potential dependencies of the normalized intensities of selected bands (Figure 13). The intensity dependencies can be divided into three groups:

1. The peaks at 1150 cm^{-1} (C–H bending), 1161 cm^{-1} (C–H bending in a semiquinonoid structure), 1417 cm^{-1} (C~N stretching in a highly localized polaron structures) and 1457 cm^{-1} (C=N stretching) reach maximum intensity around 0.2 V (Figure 13a). These bands are connected with the semiquinonoid-charged linear AO.
2. The intensity of the peaks at 1184 cm^{-1} (C–H stretching in charged linear chain), 1569 cm^{-1} (benzenoid ring stretching in linear chains), 1594 cm^{-1} (semiquinonoid ring stretching) and 1627 cm^{-1} (quinonoid ring stretching) reach their maximum around 0.4 V (Figure 13b). These bands are connected with the quinonoid-charged linear AO.
3. The intensity of the peaks at 1345 cm^{-1} (C~N stretching in delocalized polaron structure), 1373 cm^{-1} (C~N structure in localized polaron structure), 1394 cm^{-1} (C~N stretching in polaron pair structure), 1481 cm^{-1} (C=N stretching) and 1517 cm^{-1} (N–H deformation vibrations) decrease around 0.2 V (Figure 13c). These bands are connected with the *N*-phenylphenazinium-based AO.

The changes in band intensities are hugely influenced by the fact that Raman scattering from the *N*-phenylphenazinium cation-based structure is enhanced at gold SERS substrates at 633 nm excitation,

and thereby it dominates the spectrum when present in this form—below 0.2 V. The intensity changes above this point are mainly due to the redox changes of the linear AOs, always present in the mix.

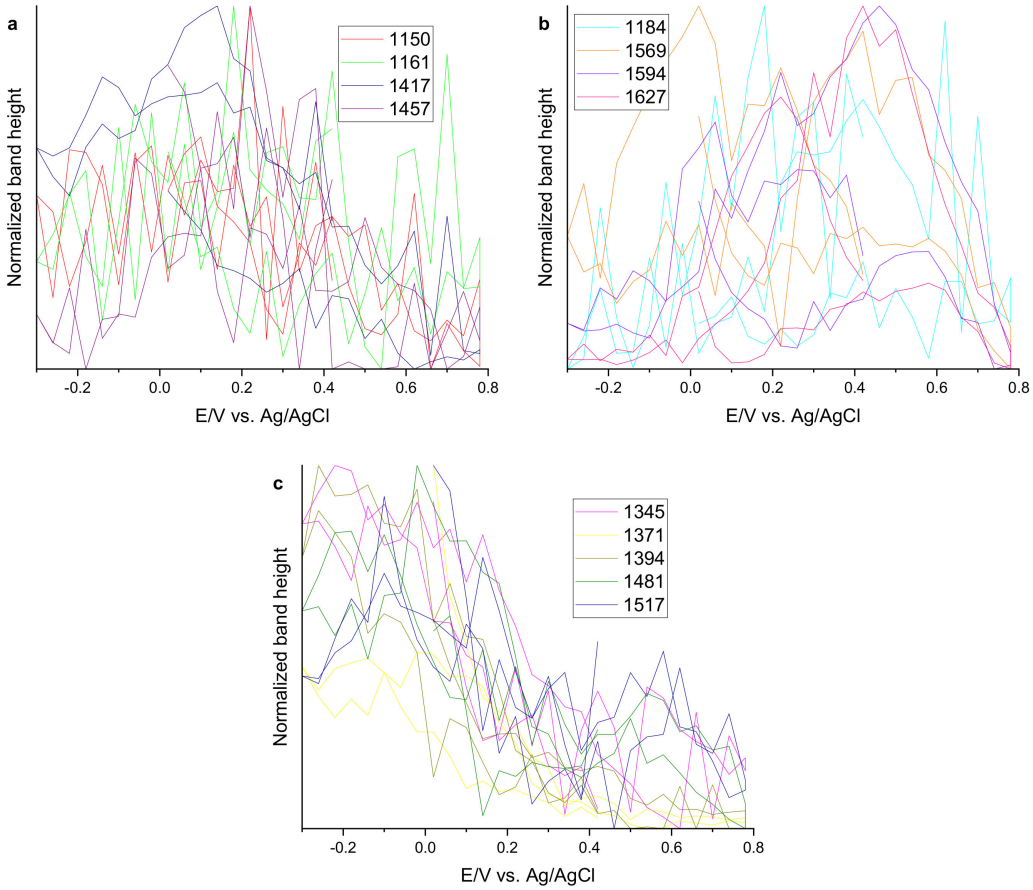

Figure 13. Potential dependencies of the normalized intensities of selected bands of semiquinonoid-charged linear AO (**a**), quinonoid-charged linear AO (**b**), and N-phenyl phenazinium-based AO (**c**) during the spectroelectrochemical study at pH 1 of the aniline oligomer (AO) formed by electrochemical oxidation of aniline in aqueous medium of pH 7. Excitation 633 nm.

4. Discussion

The chemical oxidation of aniline at starting pH 1 and 7 was followed by temperature, pH, OCP, FTIR in situ; UV–Vis and SERS ex situ.

The oxidation of aniline in acidic medium is already quite well known [24]. After mixing the aniline and APS solutions, an induction period of ca 3 min takes place. Formation of linear AOs in the oxidized state is observed by FTIR and SERS. Then the reaction rate increases, and the propagation of the pernigraniline chain is observed by all methods. After ca 15 min, pernigraniline is reduced to emeraldine, as again observed by all methods. What is important, a well-adhering PANI film is formed, but no *N*-phenylphenazinium or benzoquinone-based structures are observed at any stage of the chemical aniline oxidation started at pH 1.

These structures are not necessary for the PANI film formation, and they are also not an inherent part of the process of chemical oxidation of aniline. The aniline couples strictly in the *para* positions, resulting in a linear polymer at low pH, as proposed earlier [16,17,19,22].

The oxidation of aniline at neutral starting pH was studied before in a couple of studies [24,37]. In this case, sodium sulfate salt was added to the reaction medium to ensure conductivity for the comparable electrochemical experiment. The reaction started immediately, as can be seen from temperature, pH and OCP kinetics. UV—Vis spectroscopy detected only *N*-phenylphenazinium-based

AOs after 100 s of reaction and later on. FTIR spectra of the reaction products remained unchanged during the reaction, and phenazine-like AOs were observed throughout the whole reaction time. Their protonation state cannot be identified from the FTIR spectra. Only in the first seconds, carbonyl groups were observed.

SERS, on the other hand, detected enormous changes during the aniline oxidation in the neutral medium: In the first seconds, linear AOs were observed. After 100 s, *N*-phenylphenazinium cation and benzoquinone units absolutely dominated the spectrum. Later on, linear chain growth was observed in addition to the *N*-phenylphenazinium cation-based AOs formation. It needs to be mentioned that neutral phenazine-like AOs do not produce well-resolved Raman spectra. A fluorescence background makes them virtually impossible to analyse with Raman spectroscopy. Once they become protonated, forming the *N*-phenylphenazinium cation, SERRS enhancement of these units becomes operative.

From our observations we can conclude that *N*-phenylphenazinium-based AOs are by far the most dominant products of the reaction. However, they do not become protonated straight away. The protonation takes place after ca 100 s, which corresponds to pH 5.5, according to the pH kinetics. Linear chain and benzoquinone-based AOs are minor components in the AO mixture.

The comparison between the chemical and electrochemical oxidation of aniline is based on SERS experiments. The in-situ SERS spectroelectrochemistry at pH 1 was published earlier [18]. Here, we present an in-situ SERS spectroelectrochemical study of the aniline oxidation at pH 7; and behavior of the formed product in a medium of pH 1. The material formed on the electrode at pH 7 is not very electroactive, wherein only weak redox features of the linear AO fraction was observed. The SERS spectra of the material lack any distinguishable/significant features. The spectra also did not change very much with potential; the changes can be assigned to the linear AO fraction. In addition, the spectra were obscured by fluorescence, which is typical for the neutral form of the *N*-phenyl phenazine structure. However, after the change of the electrolyte to acidic medium (0.1 M sulfuric acid), both CV and Raman spectra changed radically as the AOs became protonated. Typical *N*-phenylphenazinium Raman features were observed below ca 0.2 V. At this potential, the *N*-phenylphenazinium cations become oxidized, and their Raman scattering is not enhanced any more. Above this potential, the linear AO fraction dominates the Raman spectrum.

5. Conclusions

We have demonstrated that *N*-phenylphenazinium cation-based AOs do not form at low pH in any amount, not even during the chemical oxidation of aniline. *N*-phenylphenazinium cation-based AOs are thus not an inherent part of the chemical oxidation of aniline. This makes the in-situ chemical preparation of PANI films equal to the electrochemical PANI film formation concerning the linearity of the PANI chains.

The *N*-phenyl phenazine-based AO was the main product of both the chemical and electrochemical oxidation of aniline at pH 7. When protonated, the *N*-phenylphenazinium cation-based AO becomes electroactive, non-fluorescent and SERS-enhanced. In the chemical oxidation of aniline started at pH 7, the protonation of the *N*-phenyl phenazine structure becomes protonated after ca 100 s, where after the pH drops to ca 5.5. The electrochemical aniline oxidation proceeds at constant pH, so the formed AO layer does not become protonated during formation in neutral medium. When protonated artificially by the change of electrolyte to 0.1 M sulfuric acid, the *N*-phenylphenazinium cation was detected. As the *N*-phenyl phenazine-based AO was protonated and electroactive, its electrochemical behavior could be studied.

It has one oxidation peak at ca 0.2 V. Below this potential, *N*-phenylphenazinium cation-based AOs are observed by SERRS. Above this potential, the SERRS enhancement of the phenazine-like AOs is turned off; leading to the dominance of the linear AO fraction in the Raman spectra.

Author Contributions: The investigation was conducted by all of the authors; the manuscript was written mainly by Z.M. All authors have read and agreed to the published version of the manuscript.

Funding: This research was funded by the Czech Science Foundation; grant number 18-01924Y.

Conflicts of Interest: The authors declare no conflict of interest.

References

1. Nasar, A.; Mashkoor, F. Application of polyaniline-based adsorbents for dye removal from water and wastewater—A review. *Environ. Sci. Pollut. Res.* **2019**, *26*, 5333–5356. [CrossRef] [PubMed]
2. Escandari, E.; Kosari, M.; Farahani, M.H.D.A.; Khiavi, N.D.; Saeedikhani, M.; Katal, R.; Zarinejad, M. A review on polyaniline-based materials applications in heavy metals removal and catalytic processes. *Separ. Purif. Tech.* **2020**, *231*, 1–27. [CrossRef]
3. Sinha, A.; Kalambate, P.K.; Mugo, S.M.; Kamau, P.; Chen, J.; Jain, R. Polymer hydrogel interfaces in electrochemical sensing strategies: A review. *TrAC* **2019**, *118*, 488–501.
4. Shoaie, N.; Daneshpour, M.; Azimzadeh, M.; Mahshid, S.; Khoshfetrat, S.M.; Jahanpeyma, F.; Gholaminejad, A.; Omidfar, K.; Foruzandeh, M. Electrochemical sensors and biosensors based on the use of polyaniline and its nanocomposites: A review on recent advances. *Microchim. Acta* **2019**, *186*, 1–29. [CrossRef]
5. Zamani, F.G.; Moulahoum, H.; Ak, M.; Demirkol, D.O.; Timur, S. Current trends in the development of conducting polymers-based biosensors. *TrAC* **2019**, *118*, 264–276.
6. Wang, Y.; Liu, A.; Han, Y.; Li, T. Sensores based on conductive polymers and their composites: A review. *Polym. Int.* **2019**, *69*, 7–17. [CrossRef]
7. Distler, T.; Boccaccini, A.R. 3D printing of electrically conductive hydrogels for tissue engineering and biosensors—A review. *Acta Biomater.* **2020**, *101*, 1–13. [CrossRef]
8. Zare, E.N.; Makvandi, P.; Ashtari, B.; Rossi, F.; Motahari, A.; Perale, G. Progress on conductive polyaniline-based nanocomposites for biomedical applications: A review. *J. Med. Chem.* **2020**, *63*, 1–22. [CrossRef]
9. Cho, S.; Lee, J.S.; Joo, H. Recent developments of the solution-processable and highly conductive polyaniline composites for optical and electrochemical applications. *Polymers* **2019**, *11*, 1–17. [CrossRef]
10. Banerjee, J.; Dutta, K.; Kader, M.A.; Nayak, S.K. An overview on the recent developments in polyaniline-based supercapacitors. *Polym. Adv. Tech.* **2019**, *30*, 1902–1921. [CrossRef]
11. Liu, Z.; Yuan, X.; Zhang, S.; Wang, J.; Huang, Q.; Yu, N.; Zhu, Y.; Fu, L.; Wang, F.; Chen, Y.; et al. Three-dimensional ordered porous electrode materials for electrochemical energy storage. *NPG Asia Mater.* **2019**, *11*, 1–21. [CrossRef]
12. Luo, Y.; Guo, R.; Li, T.; Li, F.; Liu, Z.; Zheng, M.; Wang, B.; Yang, Z.; Luo, H.; Wan, Y. Application of polyaniline for Li-ion batteries, lithium-sulfur batteries, and supercapacitors. *ChemSusChem* **2019**, *12*, 1591–1611. [CrossRef] [PubMed]
13. Wang, Y.; Ding, Y.; Guo, X.; Yu, G. Conductive polymers for stretchable supercapacitors. *Nano Res.* **2019**, *12*, 1978–1987. [CrossRef]
14. Stejskal, J.; Sapurina, I. Polyaniline: Thin films and colloidal dispersions (IUPAC Technical Report). *Pure Appl. Chem.* **2005**, *77*, 815–826. [CrossRef]
15. Gvozdenović, M.M.; Jugović, B.Z.; Stevanović, J.S.; Trišović, T.L.; Grgur, B.N. Electrochemical polymerization of aniline. In *Electropolymerization*; InTech: London, UK, 2011; pp. 77–96.
16. Jangid, N.K.; Jadoun, S.; Kaur, N. A review on high-throughput synthesis, deposition of thin films and properties of polyaniline. *Eur. Polym. J.* **2020**, *125*, 1–17. [CrossRef]
17. Stejskal, J.; Trchová, M. Aniline oligomers *versus* polyaniline. *Polym. Int.* **2012**, *61*, 240–251. [CrossRef]
18. Morávková, Z.; Dmitrieva, E. The First Products of Aniline Oxidation—SERS Spectroelectrochemistry. *ChemistrySelect* **2019**, *30*, 8847–8854. [CrossRef]
19. Ćirić-Marjanović, G.; Konyushenko, E.N.; Trchová, M.; Stejskal, J. Chemical oxidative polymerization of anilinium sulfate versus aniline: Theory and experiment. *Synth. Met.* **2008**, *158*, 200–211. [CrossRef]
20. Sapurina, I.; Stejskal, J. The mechanism of the oxidative polymerization of aniline and the formation of supramolecular polyaniline structures. *Polym. Int.* **2008**, *57*, 1295–1325. [CrossRef]
21. Gospodinova, N.; Terlemezyan, L. Conducting polymers prepared by oxidative polymerization: Polyaniline. *Prog. Polym. Sci.* **1998**, *23*, 1443–1484. [CrossRef]

22. Ćirić-Marjanović, G. Recent advances in polyaniline research: Polymerization mechanisms; structural aspects; properties and applications. *Synth. Met.* **2013**, *177*, 1–47. [CrossRef]
23. Ferreira, D.C.; Pires, J.R.; Temperini, M.L.A. Spectroscopic characterization of oligoaniline microspheres obtained by an aniline-persulfate approach. *J. Phys. Chem. B* **2011**, *115*, 1368–1375. [CrossRef] [PubMed]
24. Stejskal, J.; Sapurina, I.; Trchová, M.; Konyushenko, E.N. Oxidation of aniline: Polyaniline granules; nanotubes; and oligoaniline microspheres. *Macromolecules* **2008**, *41*, 3530–3536. [CrossRef]
25. Stejskal, J.; Sapurina, I.; Trchová, M. Polyaniline nanostructures and the role of aniline oligomers in their formation. *Prog. Polym. Sci.* **2010**, *35*, 1420–1482. [CrossRef]
26. Sapurina, I.; Ochsadev, A.Y.; Volchek, B.Z.; Trchová, M.; Riede, A.; Stejskal, J. In-situ polymerized polyaniline films: 5. Brush-like chain ordering. *Synth. Met.* **2002**, *129*, 29–37. [CrossRef]
27. Tomšík, E.; Morávková, Z.; Stejskal, J.; Trchová, M.; Zemek, J. In situ polymerized polyaniline films: The top and the bottom. *Synth. Met.* **2012**, *162*, 2401–2405. [CrossRef]
28. Trchová, M.; Morávková, Z.; Dybal, J.; Stejskal, J. Detection of aniline oligomers on polyaniline–gold intarface using resonance Raman scattering. *ACS Appl. Mater. Interfaces* **2014**, *6*, 942–950. [CrossRef]
29. Morávková, Z.; Stejskal, J.; Trchová, M. Spectrodcopic study of the highly homogeneous polyaniline film formation on gold support. *Spectrochim. Acta Part. A* **2016**, *152*, 294–303. [CrossRef]
30. Dinh, H.N.; Ding, J.; Xia, S.J.; Birss, V.I. Multi-technique study of the anodic degradation of polyaniline films. *J. Electroanal. Chem.* **1998**, *459*, 45–56. [CrossRef]
31. Gao, P.; Gosztola, D.; Weaver, M.J. Surface-enhanced Raman spectroscopy as a probe of electroorganic reaction pathways. 2. Ring coupling mechanisms during aniline oxidation. *J. Phys. Chem.* **1989**, *93*, 3753–3760. [CrossRef]
32. Dmitrieva, E.; Dunsch, L. How linear is "linear" polyaniline? *J. Phys. Chem. B* **2011**, *115*, 6401–6411. [CrossRef] [PubMed]
33. Li, R.L.; Lin, C.-W.; Shao, Y.; Chang, C.W.; Yao, F.-K.; Kowal, M.D.; Wang, H.; Yeung, M.T.; Huang, S.-C.; Kaner, R.B. Characterization of aniline tetramer by MALDI TOF mass spectrometry upon oxidative and reductive cycling. *Polymers* **2016**, *8*, 1–11. [CrossRef] [PubMed]
34. Holze, R. Adsorption of aniline on gold: A SERS study. *J. Electroanal. Chem.* **1988**, *250*, 143–157. [CrossRef]
35. Šeděnková, I.; Trchová, M.; Stejskal, J. In Situ Infrared Spectroscopy of Oligoaniline Intermediates Created under Alkaline Conditions. *J Phys. Chem. B* **2014**, *118*, 14972–14981.
36. Liu, Y.C.; Wang, C.C.; Tsai, C.E. Effects of electrolytes used in roughening gold substrates by oxidation–reduction cycles on surface-enhanced Raman scattering. *Electrochem. Commun.* **2005**, *7*, 1345–1350. [CrossRef]
37. Trchová, M.; Šeděnková, I.; Konyushenko, E.N.; Stejskal, J.; Holler, P.; Ćirić-Marjanović, G. Evolution of Polyaniline Nanotubes: The Oxidation of Aniline in Water. *J. Phys. Chem. B* **2006**, *110*, 9461–9468. [CrossRef]
38. Ćirić-Marjanović, G.; Trchová, M.; Konyushenko, E.N.; Holler, P.; Stejskal, J. Chemical oxidative polymerization of aminodiphenylamines. *J. Phys. Chem. B* **2008**, *112*, 6976–6987. [CrossRef]
39. Boyer, M.I.; Quillard, S.; Louarn, G.; Froyer, G.; Lefrant, S. Vibrational study of the $FeCl_3$-doped dimer of polyaniline; A good model compound of emeraldine salt. *J. Phys. Chem. B* **2000**, *104*, 8952–8961. [CrossRef]
40. Ping, Z. In situ FTIR-attenuated total reflection spectroscopic investigations on the base-acid transitions of polyaniline. Base-acid transition in the emeraldine form of polyaniline. *J. Chem. Soc. Faraday Trans.* **1996**, *92*, 3063–3067. [CrossRef]
41. Silva, C.H.B.; Ferreira, D.C.; Ando, R.A.; Temperini, M.L.A. Aniline-1.;4-benzoquinone as a model system for the characterization of products from aniline oligomerization in low acidic media. *Chem. Phys. Lett.* **2012**, *551*, 130–133. [CrossRef]
42. Surwade, S.P.; Dua, V.; Manohar, N.; Manohar, S.K.; Beck, E.; Ferris, J.P. Oligoaniline intermediates in the aniline-peroxydisulfate system. *Synth. Met.* **2009**, *259*, 445–455. [CrossRef]
43. Socrates, G. *Infrared and Raman Characteristic Group Frequencies*; Wiley: New York, NY, USA, 2001.
44. Šeděnková, I.; Trchová, M.; Stejskal, J. Thermal degradation of polyaniline films prepared in solutions of strong and weak acids and in water—FTIR and Raman spectroscopic studies. *Polym. Degrad. Stab.* **2008**, *93*, 2147–2157. [CrossRef]
45. Trchová, M.; Stejskal, J. Polyaniline: The infrared spectroscopy of conducting polymer nanotubes (IUPAC Technical Report). *Pure Appl. Chem.* **2011**, *83*, 1803–1817. [CrossRef]

46. Boyer, M.I.; Quillard, S.; Rebourt, E.; Louarn, G.; Buisson, J.P.; Monkman, A.; Lefrant, S. Vibrational analysis of polyaniline: A model compound approach. *J. Phys. Chem. B* **1998**, *102*, 7382–7392. [CrossRef]
47. Ping, Z.; Nauer, G.E.; Neugebauer, H.; Theiner, J.; Neckel, A. Protonation and electrochemical redox doping processes of polyaniline in aqueous solutions: Investigations using in situ FTIR-ATR spectroscopy and a new doping system. *J. Chem. Soc. Faraday Trans.* **1997**, *93*, 121–129. [CrossRef]
48. Cao, Y. Spectroscopic studies of acceptor and donor doping of polyaniline in the emeraldine base and pernigraniline forms. *Synth. Met.* **1990**, *35*, 319–332. [CrossRef]
49. Quillard, S.; Louarn, G.; Buisson, J.P.; Boyer, M.; Lapkowski, M.; Pron, A.; Lefrant, S. Vibrational spectroscopic studies of the isotope effects in polyaniline. *Synth. Met.* **1997**, *84*, 805–806. [CrossRef]
50. Huang, W.S.; MacDiarmid, A.G. Optical properties of polyaniline. *Polymer* **1993**, *34*, 1833–1845. [CrossRef]
51. Xia, Y.; Weisinger, J.M.; MacDiarmid, A.G. Camphorsulfonic acid fully doped polyaniline emeraldine salt: Conformations in different solvents studied by an ultraviolet/visible/neer-infrared spectroscopic method. *Chem. Mater.* **1995**, *7*, 443–445. [CrossRef]
52. Folch, S.; Régis, A.; Gruger, A.; Colomban, P. Chain length effect on intrachain electronic excitaion and interchain coupling in poly- and oligoanilines. *Synth. Met.* **2000**, *110*, 219–227. [CrossRef]
53. Gruger, A.; El Khalki, A.; Colomban, P. Protonation.; sol formation and precipitation of poly- and oligoanilines. *J. Raman Spectrosc.* **2003**, *34*, 438–450. [CrossRef]
54. Bilal, S.; Holze, R. In situ UV–vis spectroelectrochemistry of poly (*o*-phenylenediamine-co-*m*-toluidine). *Electrochim. Acta* **2007**, *52*, 5346–5356. [CrossRef]
55. Ding, Z.; Sanchez, T.; Labouriau, A.; Iyer, S.; Larson, T.; Currier, R.; Zhao, Y.; Yang, D. Characterisation of reaction intermediate aggregates in aniline oxidative polymerization at low proton concentracion. *J. Phys. Chem. B* **2010**, *114*, 10337–10346. [CrossRef] [PubMed]
56. Dmitrieva, E.; Harima, Y.; Dunsch, L. Influence of Phenazine Structure on Polaron Formation in Polyaniline: In Situ Electron Spin Resonance-Ultraviolet/Visible-Near-Infrared Spectroelectrochemical Study. *J. Phys. Chem. B* **2009**, *113*, 16131–16141. [CrossRef]
57. Louarn, G.; Lapkowski, M.; Quillard, S.; Pron, A.; Buisson, J.P.; Lefrant, S. Vibrational properties of polyaniline-isotope effects. *J. Phys. Chem.* **1996**, *100*, 6998–7006. [CrossRef]
58. Cochet, M.; Louarn, G.; Quillard, S.; Boyer, M.I.; Buisson, J.P.; Lefrant, S. Theoretical and experimental vibrational study of polyaniline in base forms: Non-planar analysis. Part I. *J. Raman Spectrosc.* **2001**, *31*, 1029–1039. [CrossRef]
59. de Santana, H.; Quillard, S.; Fayad, E.; Louarn, G. In situ UV-vis and Raman spectroscopic studies of the electrochemical behavior of N,N′-diphenyl-1,4-phenylenediamine. *Synth. Met.* **2006**, *156*, 81–85. [CrossRef]
60. Wojciechowski, P.M.; Zierkiewicz, W.; Michalska, D.; Hobza, P. Electronic structures; vibrational spectra; and revised assignment of aniline and its radical cation: Theoretical study. *J. Chem. Phys.* **2003**, *118*, 10900–10911. [CrossRef]
61. Cochet, M.; Louarn, G.; Quillard, S.; Buisson, J.P.; Lefrant, S. Theoretical and experimental vibrational study of emeraldine in salt form. Part II. *J. Raman Spectrosc.* **2000**, *31*, 1041–1049. [CrossRef]
62. Panicker, C.Y.; Varghese, H.M.; Anto, P.L.; Daizy, P.J. Potential dependent SERS profile of sulfanilic acid on silver electrode. *J. Raman Spectrosc.* **2006**, *37*, 853–857. [CrossRef]
63. Ćirić-Marjanović, G.; Trchová, M.; Stejskal, J. The oxidative polymerization of aniline in water: Raman spectroscopy. *J. Raman Spectrosc.* **2008**, *39*, 1375–1387. [CrossRef]
64. Anto, P.L.; Panicker, C.Y.; Varghese, H.T.; Philip, D.J. Potential-dependent SERS profile of orthanilic acid on silver electrode. *J. Raman Spectrosc.* **2006**, *37*, 1265–1271. [CrossRef]
65. Sestrem, R.H.; Ferreira, D.C.; Landers, R.; Temperini, M.L.A.; do Nascimento, G.M. Synthesis and spectroscopic characterisation of polymer and oligomers of o-phenylenediamine. *Eur. Polym. J.* **2010**, *46*, 484–493. [CrossRef]
66. Morávková, Z.; Dmitrieva, E. Structureal changes in polyaniline near the middle oxidation peak studied by in situ Raman spectroelectrochemistry. *J. Raman Spectrosc.* **2017**, *48*, 1229–1234. [CrossRef]
67. Furukawa, Y.; Ueda, F.; Hyodo, Y.; Harada, I.; Nakajima, T.; Kawagoe, T. Vibrational spectra and structure of polyaniline. *Macromolecules* **1988**, *21*, 1297–1305. [CrossRef]
68. Malinowski, E.R.; Cox, R.A.; Haldna, U.L. Factor analysis for isolation of the Raman spectra of aqueous sulfuric acid components. *Anal. Chem.* **1984**, *56*, 778–781. [CrossRef]

69. Colomban, P.; Folch, S.; Gruger, A. Vibrational study of short-range order and structure of polyaniline bases and salts. *Macromolecules* **1999**, *32*, 3080–3092. [CrossRef]
70. Brolo, A.G.; Sanderson, A.C. Surface-enhanced Raman scattering (SERS) from a silver electrode modified with oxazine 720. *Can. J. Chem.* **2004**, *82*, 1474–1480. [CrossRef]
71. do Nascimento, G.M.; Silva, C.H.B.; Temperini, M.L.A. Electronic structure and doping behavior of PANI-NSA nanofibers investigated by resonance Raman spectroscopy. *Macromol. Rapid Commun.* **2006**, *27*, 255–259. [CrossRef]
72. do Nascimento, G.M.; Pereira da Silva, J.E.; Cordoba de Torresi, S.I.; Temperini, M.L.A. Comparison of Secondary Doping and Thermal Treatment in Poly (diphenylamine) and Polyaniline Monitored by Resonance Raman Spectroscopy. *Macromolecules* **2002**, *35*, 121–125. [CrossRef]
73. Takahashi, M.; Goto, M.; Ito, M. Surface-enhanced Raman scattering of phenazine. Large intensities of overtones and combination bands. *Chem. Phys. Lett.* **1985**, *121*, 458–493. [CrossRef]